

Room temperature magnetoelectric control of micromagnetic structure in iron garnet films

A. S. Logginov,¹ G. A. Meshkov,¹ A. V. Nikolaev,¹ E. P. Nikolaeva,¹ A. P. Pyatakov,^{1,a)} and A. K. Zvezdin²

¹Department of Physics, M. V. Lomonosov Moscow State University, Leninskie gori, Moscow 119992, Russia

²A. M. Prokhorov General Physics Institute, 38, Vavilova St., Moscow 119991, Russia

(Received 10 April 2008; accepted 14 October 2008; published online 7 November 2008)

The effect of magnetic domain wall motion induced by electric field is observed in epitaxial iron garnet films grown on (210) and (110) gadolinium-gallium garnet substrates. The displacement of the domain wall changes to the opposite at the reversal of electric field polarity, and it is independent of the magnetic polarity of the domains. Dynamic observation of the domain wall motion in 400 V electric pulses gives the domain wall velocity of about 50 m/s. The same velocity is achieved in a magnetic field pulse of about 50 Oe. This type of magnetoelectric effect is implemented in single phase material at room temperature. © 2008 American Institute of Physics.

[DOI: [10.1063/1.3013569](https://doi.org/10.1063/1.3013569)]

The conventional means of data writing based on generation of magnetic field with electric current put the limit for high storage density due to the increasing energy losses.¹ Magnetization control by spin-polarized current also requires large current densities of 10^6 – 10^7 A/cm².¹ The alternative way of magnetic writing that does not involve charge or spin carrier transport is based on the magnetoelectric effect.^{2,3} It arises from the coupling between magnetic and electric subsystems in medium. There were reports on various means of electric field control of magnetism,^{4–10} but all of them have at least one of the following limitations.

- Magnetoelectric properties in semiconductors⁴ and in the majority of multiferroic materials^{5–7} appear at low temperatures.
- Few room temperature magnetoelectrics are commonly antiferromagnetic materials; thus their magnetic properties are compensated. Special exchange coupled antiferromagnetic/ferromagnetic structure is needed to convert electrical switching of antiferromagnetic order parameter into magnetization switching.⁸
- In artificial magnetoelectric materials (composites) the electric and magnetic subsystems are spatially separated.^{9,10} The dependence of the coupling between two subsystems on the conditions at the interfaces and their local variations results in the unpredictable character of magnetization switching⁹ and intricate magnetic stripe domain pattern.¹⁰

In Ref. 11 we proposed a way to control magnetization in single phase material at room temperature by using electric field only, not implying magnetic field or charge carrier transport. This sort of magnetoelectric effect appeared in iron garnet films as magnetic domain wall displacement induced by static electric field.

In this letter the effective magnetic field quantitatively characterizing the effect is estimated by dynamic measurements in pulsed electric field. We also show that magnetic

anisotropy of iron garnet film plays the crucial role in the existence of magnetoelectric effect.

Epitaxial films of iron garnets are classical magneto-optical materials and the model object to study micromagnetism.^{12,13} The electromagneto-optical effect observed in iron garnet films¹⁴ served as an indirect proof for their salient magnetoelectric properties. In our experiments we used (BiLu)₃(FeGa)₅O₁₂ iron garnet films grown by liquid-phase epitaxy on (111), (110), and (210) Gd₃Ga₅O₁₂ substrates at a growth temperature of 690 °C (for details see Ref. 15 and references therein). The surface and sectional morphologies of the films were studied using a scanning electron microscope JSM-6460LV in low vacuum backscattered electron mode. It shows that the film is a single crystal without crystallites. The chemical composition of the magnetic films was examined at different points of the cross section, and no dependence on the distance from the substrate was observed. The root mean square roughness values of the film surface measured by scanning probe microscope FemtoScan in contact mode were less than 3 nm.

The parameters of the samples are listed in Table I. In contrast to the (111) films in which both the cubic anisotropy and growth induced anisotropy assign the easy axis along the normal to the surface of the film,¹² the characteristic feature

TABLE I. Parameters of the samples under study and magnetoelectric control effect registration marks. The symbol h stands for the thickness of the iron garnet film, M_s is the saturation magnetization, p is a period of domain structure, and $(\theta; \varphi)$ are angular coordinates of the magnetic easy axis in the coordinate system with the direction normal to the film as the z -axis, and $[\bar{1}10]$ and $[\bar{1}20]$ as the x -axes for (111) and (210) films, respectively (data adopted from Ref. 15). At the right column the presence/absence of the magnetic domain wall displacement in electric field is indicated.

Sample No.	Substrate orientation	h (μm)	$4\pi M_s$ (G)	p (μm)	(θ, φ) (deg)	Effect detection
1	(111)	8.5	63	77	(0, 0)	No
2	(111)	19	78	39	(0, 0)	No
3	(110)	4	162	9.2	(10, -53)	Yes
4	(110)	6	76	14	(10, 1.5)	Yes
5	(210)	7.4	77	44	(46, 207)	Yes
6	(210)	10	62	28	(46, 189)	Yes
7	(210)	10	53.5	34	(40, 189)	Yes

^{a)}Author to whom correspondence should be addressed. Electronic address: pyatakov@phys.msu.ru and alpya@newmail.ru. Tel.: +7-495-939-4138.

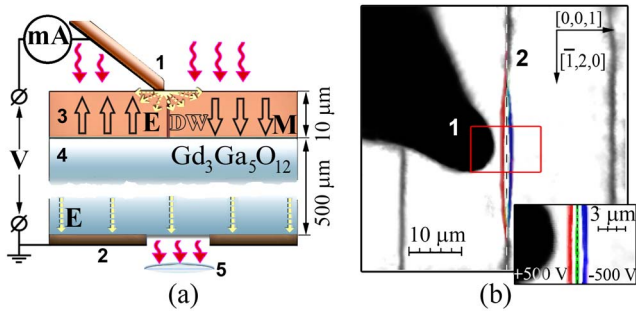


FIG. 1. (Color online) The magnetic domain wall displacement in electric field. (a) Schematic representation of the geometry of the experiment and the configurations of the electric field and magnetization. The electric field (the field lines are shown by the dashed lines) is formed in the dielectric medium of the sample between the tip (1) and the copper foil (2), which plays the role of the grounding electrode. The maximum field strength (about 800 kV/cm) is reached in the iron garnet film (3) near the tip at the voltage of 500 V applied; it decreases rapidly in the bulk of $\text{Gd}_3\text{Ga}_5\text{O}_{12}$ substrate (4) and does not exceed 500 V/cm near the grounding electrode (2). The absence of the leakage currents is controlled with the milliamperemeter (mA). The incident light (denoted with wavy arrows) is along the normal to the surface. The objective lens (5) is placed behind the pinhole in the foil (2). In the magnetic film (3) the domains and domain wall (DW) are schematically shown. (b) Magneto-optical images of domain walls at the tip electrode potentials of +500 and -500 V superimposed on each other. In the vicinity of tip electrode (1) the segment of domain wall (2) is attracted to the tip at a positive potential of +500 V (red) and is repelled by the tip at a negative potential of -500 V (blue). The equilibrium position of the domain wall is shown by the dashed line. Three positions of the wall in selected area (from left to right: +500, 0, and -500 V) are shown in the inset. In (210) films the domain walls have the tendency to orient along the $[\bar{1}20]$ crystallographic direction. Sample 7 from Table I was used.

of (110) and (210) samples was the considerable deviation of the easy axis from the normal due to the misalignment of the growth direction and $[111]$ cubic easy axis.¹⁵

To produce a high-strength electric field in the dielectric iron garnet film, we used a 50 μm diameter copper wire with a pointed tip, which touched the surface of the sample in the vicinity of the domain wall [Fig. 1(a)]. The tip curvature radius of the copper “needle” was about 5 μm . This allowed us to obtain an electric field strength of up to 1000 kV/cm near the tip by supplying a voltage of up to 500 V to the needle. The field caused no dielectric breakdown because it decreased rapidly with distance from the tip and, near the grounding electrode (a metal foil attached to the substrate), did not exceed 500 V/cm. The absence of the possible leakage currents between the tip and the grounding electrode (e.g., along the sample surface) was verified by a milliamperemeter. The magneto-optical technique in Faraday geometry was used to observe the micromagnetic structure through a pinhole with the diameter of ~ 0.3 mm that was made in the grounding electrode. The image of the magnetic structure was taken by a charge coupled device camera.

In static measurements we register the magnetization distribution in initial state, and the position of domain wall with static electric field applied. Typical images illustrating the local displacement of the domain wall in the vicinity of the tip under electric field are shown in Fig. 1(b). The direction of the displacement was opposite for opposite polarities of the tip. As soon as the dc voltage was switched off, the domain walls came back to the equilibrium position. This effect of electric field controlled domain wall position was observed in iron garnet films with (210) and (110) substrate orientations and was not observed in (111) films (see Table I,

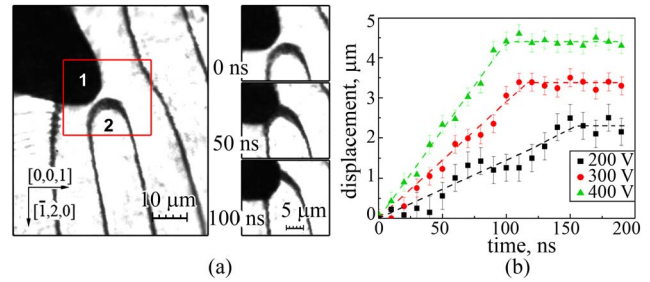


FIG. 2. (Color online) Dynamic measurements of the domain wall displacement in iron garnet films under a steplike voltage pulse of +400 V (duration of 300 ns and rise time of 20 ns). Sample 6 from Table I was used. (a) The initial micromagnetic configuration: (1) is the tip electrode and (2) is the stripe domain head. Photos of selected area show the consecutive stripe domain head positions: before electric pulse (0 ns) and instantaneous position of the domain wall moving in electric field pulse (50 ns from the start of the pulse), at ultimate equilibrium position in electric field (100 ns from the pulse start). The broadening of stripe domain head images is a characteristic feature of (210) films caused by the tilt of the easy axis from the normal to the film surface. (b) The dots on graphs show the domain wall displacement vs time for pulses with voltages of 200 V (black squares), 300 V (red circles), and 400 V (green triangles). The dashed lines are interpolation of the dependences. The linear fit of ascending sections of the curves gives the values of the velocities of 14 ± 3 , 29 ± 5 , and 44 ± 4 m/s for 200, 300, and 400 V, respectively. The large dispersion of experimental points for dynamic dependences in low field (200 V) probably is related to domain wall pinning at the defects.

note that to illustrate the idea, Table I lists the most representative examples while much more samples were tested to verify the dependence on substrate orientation). The most prominent changes were observed in (210) films at stripe domain heads [Fig. 2(a)]. The reversible domain wall displacements of up to 5 μm were detected. At higher values of displacement the modification of the micromagnetic structure had irreversible character.

For dynamic measurements the high speed photography technique was used:¹⁶ the pulses of electric field (pulse width of ~ 300 ns and rise time of ~ 20 ns) were followed by pulses of laser illumination (duration of ~ 10 ns) to get an instantaneous image of the structure under the influence of electric field. Varying the time delay between field and laser pulses enabled us to observe the consecutive positions of domain wall and thus investigate its dynamics. In the dynamic measurements the amplitude of voltage pulses was up to 400 V.

The results of dynamic measurements are shown in Fig. 2. In response to the applied electric field, the domain wall steadily moves until it reaches the equilibrium position corresponding to the field applied [the consecutive positions of stripe domain head are shown in Fig. 2(a)]. Both the values of domain wall velocity and the ultimate displacement of domain wall increase with the value of electric field [Fig. 2(b)], but the first value is a more adequate characteristic of the effect as it depends on the mobility of the wall (which can be easily measured in pulse magnetic field), while the latter one is determined by long range magnetostatic forces and their accounting requires complex micromagnetic calculations.

To compare the velocities achieved in electric field with typical velocities of domain wall in magnetic field, we carried out the measurements in magnetic field pulses. The velocity of 50 m/s similar to the one obtained in a voltage pulse of 400 V (electric field at the tip $E=400$ V/5 μm

=800 kV/cm) was achieved in a pulse magnetic field of about 50 Oe.

We point out several characteristic features of the phenomenon, which serve as the basis for the following discussion.

- (i) The direction of the domain wall displacement depends on the polarity of the voltage (and, hence, on the direction of the electric field): in the case of positive polarity, the wall was attracted to the needle and, in the case of negative polarity, it was repelled.
- (ii) The direction of the wall displacement did not depend on the magnetic polarity of the domain over which the tip was located.
- (iii) The effect was observed in films with considerable in-plane anisotropy [the films with (210) and (110) substrate orientations] and was not observed in highly symmetrical (111) films.

The influence of electric field on the micromagnetic structure was predicted theoretically in a series of works.^{17–22} These theoretical models took into account the so-called *inhomogeneous magnetoelectric interaction* that gives rise to electric polarization associated with magnetic inhomogeneities. From this point of view such spatially modulated magnetic structures as magnetic domain walls,^{17,20} spin cycloids,^{18,19} magnetic vortices,²¹ and vertical Bloch lines²² were considered, and it was shown that various electric charge distributions are associated with them.

The inhomogeneous magnetoelectric effect corresponds to the special contribution to the free energy of the crystal that takes the following high symmetry form for the bulk crystal of iron garnets with cubic symmetry:^{19,21}

$$F_{ME} = \gamma \cdot \mathbf{E} \cdot [\mathbf{M} \cdot (\nabla \cdot \mathbf{M}) - (\mathbf{M} \cdot \nabla)\mathbf{M}], \quad (1)$$

where $\mathbf{M}=\mathbf{M}(\mathbf{r})$ is the magnetization distribution, \mathbf{E} is the electric field, ∇ is the vector differential operator, and γ is the inhomogeneous magnetoelectric constant. One can learn immediately from Eq. (1) that the effect is odd with respect to electric field \mathbf{E} and does not change the sign with magnetization \mathbf{M} reversal, which agrees with features (i) and (ii) of the effect. Feature (iii) of the effect, i.e., the dependence on the substrate orientation, can be explained by the fact that the necessary condition for the effect is the local violation of space inversion in domain wall, i.e., the nonzero $(\nabla \cdot \mathbf{M})$ and $(\mathbf{M} \cdot \nabla)\mathbf{M}$ terms. In (111) films we deal with the Bloch-type domain walls [$(\nabla \cdot \mathbf{M})=0$ and $(\mathbf{M} \cdot \nabla)\mathbf{M}=0$], in which the space inversion symmetry characteristic for the bulk material persists and thus the electric field has no effect on domain wall. However the anisotropy of (210) and (110) samples requires the deflection of the magnetization from the normal to the film resulting in the Néel component in the domain wall: the direction of spin modulation and the direction normal to the rotation plane do not coincide anymore. This condition is expressed in mathematical form as $(\nabla \cdot \mathbf{M}) \neq 0$, $(\mathbf{M} \cdot \nabla)\mathbf{M} \neq 0$, and thus nonzero magnetoelectric terms in Eq. (1).

It is interesting to note that the electromagneto-optical effect observed on local areas was shown to occur on sites of domain wall localization.²³ Thus the transformation of micromagnetic structure observed in our experiment may be the

microscopic mechanism of the local electromagneto-optical effect.

In conclusion, the electric field control of magnetization distribution is implemented in single crystal material at room temperature not implying electric current. The effect is observed in epitaxial iron garnet films with in-plane anisotropy [grown on (210) and (110) gadolinium-gallium garnet substrates] and is not observed in high symmetry (111) films. The domain wall displacement has a reversible character in the range of 1–5 μm and irreversible one at larger distances. The average domain wall velocity of 50 m/s in 400 V voltage pulse was achieved, which was equivalent to the effect of 50 Oe magnetic field pulses. The control voltage can be scaled down to several volts by further miniaturization of the tip opening the exciting possibilities in the field of micro- and nanomagnetism.

The support of Russian Foundation for Basic Research (RFBR) Grant No. 08-02-01068-a, Dynasty Foundation, and "Progetto Lagrange-Fondazione CRT" is acknowledged. The authors are grateful to A. M. Balbashov and F. V. Lisovskii for samples provided, V. B. Mityukhlyayev for SEM characterization of the samples, and Z. A. Pyatakova for image processing and figures design.

- ¹C. Chappert, A. Fert, and F. N. Van Dau, *Nature Mater.* **6**, 813 (2007).
- ²Ch. Binek and B. Doudin, *J. Phys.: Condens. Matter* **17**, L39 (2005).
- ³M. Bibes and A. Barthélémy, *Nature Mater.* **7**, 425 (2008).
- ⁴D. Chiba, M. Sawicki, Y. Nishitani, Y. Nakatani, F. Matsukura, and H. Ohno, *Nature (London)* **455**, 515 (2008).
- ⁵M. Fiebig, Th. Lottermoser, D. Frohlich, A. V. Goltsev, and R. V. Pisarev, *Nature (London)* **419**, 818 (2002).
- ⁶E. Milov, A. Kadomtseva, G. Vorob'ev, Yu. Popov, V. Ivanov, A. Mukhin, and A. Balbashov, *JETP Lett.* **85**, 503 (2007).
- ⁷Y. Yamasaki, Y. Sagayama, H. Goto, T. Matsuura, M. Hirota, K. Arima, and T. Tokura, *Phys. Rev. Lett.* **98**, 147204 (2007).
- ⁸Y.-H. Chu, L. W. Martin, M. B. Holcomb, M. Gajek, S.-J. Han, Q. He, N. Balke, C.-H. Yang, D. Lee, W. Hu, Q. Zhan, P.-L. Yang, A. Fraile-Rodríguez, A. Scholl, Sh. X. Wang, and R. Ramesh, *Nature Mater.* **7**, 478 (2008).
- ⁹F. Zavaliche, H. Zheng, L. Mohaddes-Ardabili, S. Y. Yang, Q. Zhan, P. Shafer, E. Reilly, R. Chopdekar, Y. Jia, P. Wright, D. G. Schlom, Y. Suzuki, and R. Ramesh, *Nano Lett.* **5**, 1793 (2005).
- ¹⁰T. K. Chung, G. P. Carman, and K. P. Mohanchandra, *Appl. Phys. Lett.* **92**, 112509 (2008).
- ¹¹A. S. Logginov, G. Meshkov, A. V. Nikolaev, and A. Pyatakov, *JETP Lett.* **86**, 115 (2007).
- ¹²A. P. Malozemoff and J. C. Slonczewski, *Magnetic Domain Walls in Bubble Materials* (Academic, New York, 1979).
- ¹³A. K. Zvezdin and V. A. Kotov, *Modern Magneto-optics and Magneto-optical Materials* (IOP, Bristol, 1997).
- ¹⁴B. B. Krichevtsov, V. V. Pavlov, and R. V. Pisarev, *JETP Lett.* **49**, 535 (1989).
- ¹⁵A. M. Balbashov, A. S. Logginov, and E. P. Shabaeva, *Sov. Phys. Tech. Phys.* **36**, 680 (1991).
- ¹⁶A. S. Logginov, A. V. Nikolaev, and V. V. Dobrovitski, *IEEE Trans. Magn.* **29**, 2590 (1993).
- ¹⁷V. G. Bar'yakhtar, V. A. L'vov, and D. A. Yablonskii, *JETP Lett.* **37**, 673 (1983).
- ¹⁸Yu. Popov, A. Kadomtseva, G. Vorobev, and A. Zvezdin, *Ferroelectrics* **162**, 135 (1994).
- ¹⁹A. Sparavigna, A. Strigazzi, and A. Zvezdin, *Phys. Rev. B* **50**, 2953 (1994).
- ²⁰A. A. Khalifina and M. A. Shamtsudinov, *Ferroelectrics* **279**, 19 (2002).
- ²¹M. Mostovoy, *Phys. Rev. Lett.* **96**, 067601 (2006).
- ²²A. S. Logginov, G. A. Meshkov, A. V. Nikolaev, A. P. Pyatakov, V. A. Shust, A. G. Zhdanov, and A. K. Zvezdin, *J. Magn. Magn. Mater.* **310**, 2569 (2007).
- ²³V. E. Koronovskyy, S. Ryabchenko, and V. F. Kovalenko, *Phys. Rev. B* **71**, 172402 (2005).